Society For Biomaterials

Review Article

The need for stent–lesion matching to optimize outcomes of intracoronary stent implantation

Peter Lanzer,[1] Gerhard Strupp,[2] Wolfram Schmidt,[3] L. D. Timmie Topoleski[4]

[1]Department of Cardiology and Angiology, Hospitals and Clinics Bitterfeld-Wolfen, Bitterfeld, Germany
[2]Department of Cardiology, Klinikum Fulda, Fulda, Germany
[3]Institute of Biomedical Engineering, University of Rostock, Germany
[4]UMBC Laboratory for Implantable Materials and Biomechanics, University of Maryland, Baltimore County, Baltimore, Maryland

Received 9 December 2011; revised 1 October 2012; accepted 17 February 2013
Published online 17 May 2013 in Wiley Online Library (wileyonlinelibrary.com). DOI: 10.1002/jbmb.32956

Abstract: Intracoronary stents have markedly improved the outcomes of catheter-based coronary interventions. Intracoronary stent implantation rates of over 90% during coronary angioplasty are common. Stent implantations are associated with a small but statistically significant number of adverse outcomes including restenosis, thrombosis, strut malapposition, incomplete strut endothelialization, and various types of stenting failure. Better matching of biomechanical properties of stents and lesions could further improve the clinical outcome of intracoronary stenting. Thus, in this article, we assess the need for advanced intracoronary stent–lesion matching. We reviewed the data on biomechanics of coronary stents and lesions to develop knowledge-based rationale for optimum intracoronary stent selection. The available technical information on marketed intracoronary stents and the current understanding of the biomechanical properties of coronary lesions at rest and under stress are limited, preventing the development of knowledge-based rationale for optimum intracoronary stent selection at present. Development of knowledge-based selection of intracoronary stents requires standardization of mechanical stent testing, communication of the nonproprietary technical data on stents by the industry and dedicated research into procedural stent–lesion interactions. © 2013 Wiley Periodicals, Inc. J Biomed Mater Res Part B: Appl Biomater, 101B: 1560–1570, 2013.

Key Words: intracoronary stenting, coronary artery lesions, biomechanics, stent, lesion matching

How to cite this article: Lanzer P, Strupp G, Schmidt W, L. D. Timmie Topoleski. 2013. The need for stent–lesion matching to optimize outcomes of intracoronary stent implantation. J Biomed Mater Res Part B 2013:101B:1560–1570.

INTRODUCTION

Intracoronary stents have markedly improved the procedural outcome of catheter-based coronary interventions.[1] Intracoronary stent implantation rates of over 90% during coronary angioplasty are routine today, and the strategy of direct stenting implies implantation rates of 100%. At present, more than 200 different stent types are available for clinical intracoronary use worldwide.[2] However, clinical choices are difficult because little technical data on the mechanical behavior of stents and their interactions with the coronary artery walls are available.[3,4]

Here, we provide a brief review of the technical data on stents and the methodology to objectively asses the stent performance, along with a short introduction to the biomechanical properties of the coronary artery lesions. The success of a stent depends, in large part, on successful delivery, which in turn depends on both the stent and the lesion to which the stent has to be delivered. We thus bring together and summarize the available biomechanical and biomaterials knowledge-base available to the interventional cardiologists to make informed choices upon stents and stent delivery systems (SDSs).

INTRACORONARY STENTS

Besides sizing and pricing, the selection of intracoronary stents is based on a number of criteria including stent design and geometry, material, coating, drug loading, mode of expansion, site dedication, and other criteria. For clinical purposes, the stents can be conveniently grouped into bare-metal (BMS), drug-eluting (DES), and bioabsorbable (BAS) stents.

Based on the initial broad spectrum of designs including slotted tube, modular, multicellular modular, helical-sinusoidal, and multicellular, three basic stent types can be distinguished today: the closed cell design, the open cell design,

Correspondence to: P. Lanzer (e-mail: planzer@gzbiwo.de)

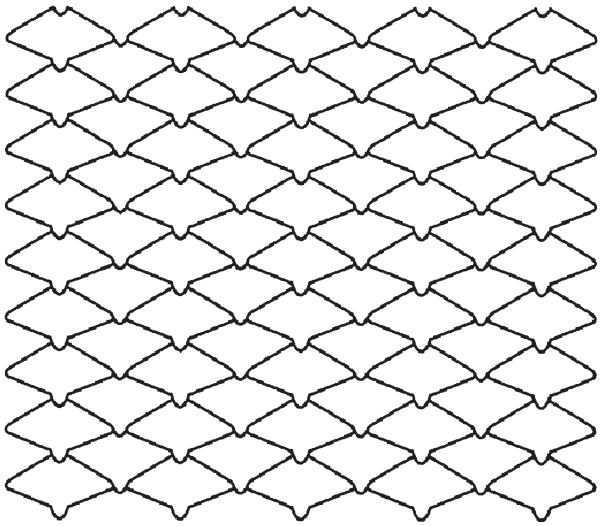

FIGURE 1. Stent with a closed cell design. Drawing of a mesh-type stents allowing homogeneous wall coverage at the cost of a lower flexibility.

and transitional forms. The closed cell design (Figure 1) improves vessel coverage at the cost of longitudinal flexibility, whereas open cell design (Figure 2) is associated with a greater flexibility and lower, but potentially inhomogeneous, vessel wall coverage, particularly around curves, harboring the hazard of plaque intrusion or distal embolization. The open cell design, also called "modular design," consists of rows of cells—termed crowns—that are longitudinally connected by links. These links can be partially corrugated (Figure 3), allowing for greater flexibility and expansibility. At present, the vast majority of BMS's are balloon expandable; more recently, however, self-expanding intracoronary stents have become available.[5]

Intracoronary stents are manufactured from nondegradable materials such as steel alloys, tantalum, cobalt alloys (Ni/Co; Co/Cr), platinum, platinum alloys (PtCr), nitinol, titanium, nickel-free alloy: for example, Biodur 108®. Bioabsorbable materials include poly-96L/4D-lactic acid (PLA), PLA-derivatives, Mg-alloy, acetylic salicylic acid (ASA), polycarbonates, hydroxyapatite, and others.

Struts are wirelines enclosing the individual stent cells; in their entirety they form the three-dimensional geometry of the stent. Initially, the struts were bulky, poorly finished wires with unfavorable deployment kinetics. Subsequently, they were refined. Better cross-sectional profiles including round, ellipsoidal, quadrangular, rectangular, and trapezoidal shapes, and better surface polish have improved deliverability and biocompatibility. The major step forward in stent design, however, was the reduction in strut diameter associated with lower restenosis rates[6] and better strut endothelial coverage.[7] The need to provide homogeneous circumferential coverage of the vessel wall to prevent protrusions of debris and distal embolizations, and the need to prevent stent recoil limit the miniaturization of strut diameters and reduction in strut density. Finding the optimum balance between these competing requirements represents an ongoing challenge to stent designers.

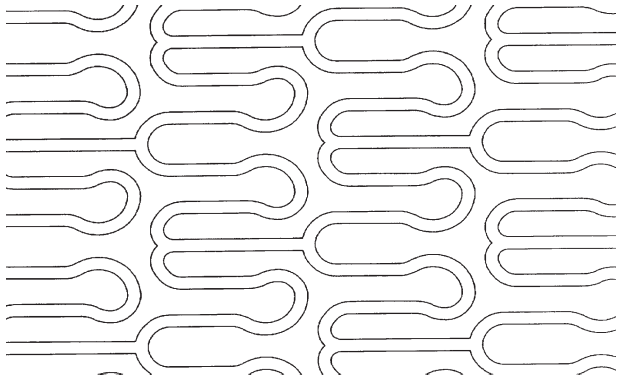

FIGURE 2. Stent with an opened cell design. Shown is a drawing of an opened cell design. Longitudinal links are reduced in number allowing more flexibility, better side branch access, but lower vessel wall coverage.

In addition to strut design, the finishes of the strut surfaces and strut coatings have been explored. Many different organic and inorganic compounds were used to coat smooth and polished struts to improve biocompatibility, including the biologically active stent (BAS) designs. Examples of biologically inert coatings include ceramic compounds, for example: Probiocoating (Prokinetic), "turbostratic" Carbon (Chrono). Biologically passive coatings include Polyzene-F (Catania), Polysaccharide (Camouflage, CC-Flex/-ProActive.), Retinoic acid (Vita-Stent), and "Hydrex"-coating (FlexMaster F1). Biologically active coatings include endothelial progenitor cell-antibody coating (Genous) or NO eluting (TITAN-2). Based on the results of numerous clinical trials, the benefits of strut coating appear questionable.

The clinical performance of intracoronary stents is also determined by the properties of the SDS. Deliverability of stents to the target sites is a complex function of the lateral flexibility and strength of the hypotube, the configuration of the transition points between the shaft and the carrier

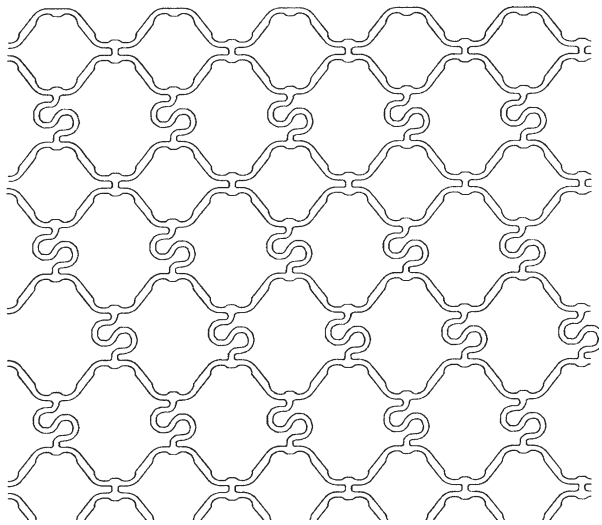

FIGURE 3. Stent with corrugated links. Corrugated links are met in open cell design, as well as in closed cell design reducing foreshortening effects at the moment of expansion.

TABLE I. Measured Stent Outer Diameter of 3.0 mm Stents at Nominal Pressure (NP), Rate Bursted Pressure (RBP), and After Subsequent Balloon Deflation (p_0) as a Measure of the Elastic Recoil

	NP (bar)	RBP (bar)	Profile at NP d(NP) (mm)	Profile After Expansion d(p_0) (mm)	Elastic Recoil (%)
Driver 3.0/15	9	16	3.225	3.042	5.67
Coroflex Blue 3.0/16	10	15	3.119	2.903	6.87
Tsunami Gold 3.0/15	10	14	3.244	3.113	4.04
Multilink Vision 3.0/15	9	16	3.294	3.115	5.45
Presillion 3.0/17	12	16	3.112	2.968	4.63
Pro-Kinetic Energy 3.0/15	9	16	3.139	2.992	4.68
Liberté 3.0/15	9	18	3.300	3.162	4.17
Titan 2 3.0/16	8	16	3.162	3.048	3.60
Blazer 3.0/15	9	16	3.283	3.131	4.65

balloon, the diameter and shape of the entry- and crossing profiles, and other factors.

Dedicated stents were designed to meet specific requirements of specific lesion types. The four major groups include (1) stents fully covered with a membrane such as polytetrafluoroethylene on a BMS, or between two layers of BMS, primarily to seal perforations or to exclude coronary aneurysms,[8] (2) stents for optimal positioning and radial support to revascularize ostial lesions, for example, using the flaring technique with a stepwise expansion of the proximal segment, followed by a flaring expansion accommodating the ostia using a distal high compliance balloon, (3) stents designed for venous graft lesions, for example, M-Guard-Stent, consisting of a nitinol nanomesh surrounding a BMS to avoid distal embolization fulfilling function similar to embolic protection devices at the price of a bulky profile and low flexibility, and (4) stents designed for bifurcations lesions. In the latter group, depending on the selected revascularization strategy, four stent types can be distinguished:

- Side-branch first
  - Tryton, Sideguard, Nile Delta, and Delta Pax
- Main-branch first
  - Stentys*, ML-Frontier, Pathfinder *(concealed wire), Twin Rail*, Nile Croco, Nile Pax*, Taxus Petal BSC*, AST SLK-view, Side-Kick, and Antares
- Simultaneous technique
  - Medtronic bifurcation system
- Noncarinal technique
  - Axxess and Axxess plus*

(*) DE properties

Side-branch first systems commit to the two stent approach, leaving no room for provisional stenting. The best validated system up to now appears the Axxess-Stent, consisting of up to three stents. Promising initial results of this device are attributed by the advocates to the specific noncarinal-touch feature of this self expanding stent.[9]

Introduction of stents with drug agents used to control myointimal hyperplasia in response to stenting-related coronary artery wall injury has markedly improved the outcome and has significantly broadened the indications.[2] Three main groups of drugs can be distinguished: (1) paclitaxel; (2) "limus" group: sirolimus, everolimus, tacrolimus, pimecrolimus, zotarolimus, Novolimus, Biolimus A9, and Myolimus; and (3) "excipients" such as ascorbylpalmitate and polvinylpyrolidone. The first generation DES were Cypher (Cordis) and Taxus (Boston Scientific), still the best clinically evaluated DES available. However, their nondegradable polymers and bulky strut design have limited their clinical performance. The second and third generations of DES brought about numerous technological improvements including lower stent profiles, decreased strut diameters and polymer thickness, struts with abluminal cavities, (e.g., Janus, Conor, and Nevo), struts holding the drugs on corrugated bare strut surfaces using van der Waal forces, biodegradable polymers, and variety of drugs with variable release kinetics. Table I provides an overview of some of the currently marketed DES scaffolds. Table A1 provides an overview of some of the biodegradable polymers in current clinical use. Table A2 gives an overview of some of the nonbiodegradable polymers in current clinical use.

Fully BAS such as Igaki Tamai, bioresorbable vascular scaffold I + II, and absorbable metal stent I + II still remain investigational. BAS with a slowly degrading PLA semicrystalline core and a faster degrading amorphous drug, containing a PLA layer, appear promising, leaving virtually no traces within the vessel wall after degradation. Other candidate substrates showing promise include PLA and its derivatives, ASA.

TABLE A1. Degradable/bioabsorbable Polymers[35]

Material		Degradation Period (Months)
DLPG	50/50 poly-D,L-lactide-*co*-glycolide	1–2
PGLA	Poly (D,L-lactide/glycolide) copolymer	2–3
PGA	Poly(glycolic acid)	2–3
DLPG	85/15 poly-D,L-lactide-*co*-glycolide	5–6
PHBV	Poly (hydroxybutyrate/hydroyvalerate) copolymer	6
PLA	Polylactic acid	9
POE	Polyorthoester	10
PLLA	Poly-L-lactic-acid	12–18
PCL	Polycaprolactone	36

TABLE A2. DES

DES with nondegradable polymers	
Cypher Select	PEVA/PBMA
Taxus Liberte	Translute
Taxus element	Translute
Coroflex please	P-matrix polysulfon
Phoenix Pico	Polysulfon
XienceV/Promus	Fluor-acryl polymer
Promus element	Fluor-acryl polymer
Xience Prime LL	Fluor-acryl polymer
Pico Elite	"Elastomer"
Angstrom III	Carbon-polymer
Firebird I	"Base and topcoating"
Endeavor Resolute	Biolinx
Irist/-small	P-5 (triflosal analogue)
DES with nondegradable "base coat" and degradable drug carrying polymer	
Nobori	Parylene + PLA
Biomatrix	Parylene + PLA
Intrepide	Parylene
DES with degradable drug carrying polymer	
Euca Tax	Camouflage + PLGA matrix
X-tent	PLA
Infinnium	Polymer mixture
Supralimus Core	Polymer mixture
Supralimus	Polymer mixture (PLG, PVP)
Mahoraba	PLGA
Genistein	Genistein multilayer
LucChopin 2	n.a.
NEVO	PLGA
Itrix	PLGA
DES with biological coating	
Endeavor Sprint	Phosphorylcholin
Zodiac	Phosphorylcholin
DES without polymer	
Yukon Choice DES	Proprietary coating
Artax	"Sinter coating"
Janus Optima	Depots
Genius-Taxcor	n.a.
Nile-Pax	n.a.
Amazonia Pax	n.a.

Performance criteria of intracoronary stent delivery systems

Technical standards describing how to measure and provide information on some of the biomechanical properties of stents and SDS have been developed.[10–12] To obtain marketing approval, manufacturers must provide the required data; however, the marketing approval practices vary among countries. Approval guidance documents are published by the United States Food and Drug Administration (FDA),[13] but not by any European Union or as far as we are aware, any other authority worldwide. Although FDA recommendations cover a wide range of biomechanical stent properties that are suggested for product characterization, they do not specify any methodology to perform the proposed measurements. Of course, to allow comparisons between products, standardized methodology of nonclinical engineering tests would be needed. Furthermore, the technical data on individual intracoronary stent products obtained by the industry and submitted to the regulatory agencies are rarely published. Stent product labeling typically includes the diameter at nominal pressure (NP), length at full expansion, compliance curve characteristics, and guide wire and guiding catheter compatibility. Even in more extensive product literature, information on biomechanical performance criteria is usually not stated. Thus, at present, the interventionalists cannot differentiate between intracoronary stents or select stents based on objective biomechanical criteria. Typical decision making criteria include evidence based on clinical trials, the interventionalists own previous experience, and the stents' cost.

Besides safety, *deliverability* of intracoronary stents to the target sites, is the key criterion of clinical utility. Deliverability—characterized by trackability, crossability, pushability, and torqueability—cannot be compared unless the user is prepared to perform direct testing.[14,15] In fact, no standardized or accepted definitions of the individual terms are available. Based on our extensive experience we have proposed the following descriptions[16]:

The *trackability* is the ability of an SDS to pass along a guiding catheter and through a curved vessel path. Low friction and smooth passage will enhance safety of application and facilitate delivery in the complex anatomy of the upstream coronary arteries and target vessels.

The *crossability* describes the propensity of an SDS to pass through a narrowing of the lumen, allowing exact positioning across the target lesion. This performance criterion is of particular importance in direct stenting.

The *pushability* is the ability to advance an SDS in coronary vessels, conveniently represented by the efficiency of transfer of the proximally applied push force, through the delivery system within the vessel path, to the distal catheter tip. The higher the ratio between distally measured and proximally applied forces, the higher pushability and greater ability to overcome obstacles. Thus, a pushability ratio of unity implies that there is no loss through the delivery path.

The *torqueability* is defined as the propensity of an SDS to tolerate torque between the proximal hub and the distal tip without kinking or other irreversible damage to the system.

To quantify the individual components of deliverability under experimental conditions, we have designed a test system that allows precise and reproducible measurements, detailed previously.[14,16] In this experimental arrangement, the mean track force is a measure of trackability and can be calculated from:

$$\text{Trackability} = \frac{1}{n}\sum_{i=1}^{n} F_{\text{prox}}(i)$$

where n is the number of force measurements along the entire travel path, and F_{prox} is the force measured at the hub of the SDS. The trackability, as a measure representing the total required physical work during advancement, is well suited for comparison between different SDS's. The recorded force–distance curves provide additional information such as peak forces at specific locations within the model, typically found at the tight curves and small radii.

Crossability of an SDS can be assessed using the same test setup, equipped with an additional load cell at the stenotic segment, simulating the target lesion. The lower the

reactive force developed during crossing of the lesion, the better the crossability. In this set up, the effects of friction along the catheter shafts and flexibility of the entire system on the crossability are minimized. The stenotic models may be selected to match the profile of the SDS or they can be specified to any given diameter. In addition, the shape and the surface morphology of model lesions can be altered. Systematic measurements have shown that, compared to BMS, the DES display poorer crossability, due mostly to larger profiles in the region of the crimped stent.[16]

Crossability of an SDS can be represented by the mean distal reaction force recorded during the passage of the balloon/stent region across the lesion and calculated from:

$$\text{Crossability} = \frac{1}{n}\sum_{i=1}^{n} F_{\text{dist}}(i)$$

where n is the number of force measurements along the entire travel path, and F_{dist} is the force measured at the tip of the SDS. To allow for accurate and reproducible comparisons of the stenosis, models must be well defined, and for a given batch of measurements, must be identical.

Pushability of an SDS can be assessed similarly to crossability, except a model of total occlusion is used instead of a stenosis, and the distal reaction force F_{dist} is measured in parallel to the proximally applied force, F_{prox}. Pushability is calculated from:

$$\text{Pushability} = \frac{F_{\text{dist}}}{F_{\text{prox}}} \cdot 100\%$$

where F_{dist} and F_{prox} have been defined above. In the proposed set up, the maximum measured proximal push forces are about 4 N, set by experience to avoid damage of the SDS during the test and assuring a quasilinear transfer function.

The torqueability can be assessed in our model by applying an increasing degree of torsion at the proximal end, up to a defined maximum. The torqueability is reported based on the state of the system after it has been torqued to rotate typically by 360 or 720°. In the case of SDS, torqueability is not only a safety issue, to avoid breaking junctions or flexible tubes, but also an issue of delivering the stent to the target site in a proper axial alignment. Quantitative measurements of the torsional transfer function can be determined by assessing the torsional moment at the hub at a given torque angle while holding the catheter tip fixed. The measurements are technically feasible but have not as yet been standardized.

In addition to deliverability of the SDS, a simple and safe retraction of the system is critical to avoid complications, such as stent deformation or strut damage. Thus, following the stent deployment, the SDS has to be withdrawn with a fully refolded dilatation balloon. Measurements of withdrawal forces can be performed by simulating stent deployment in a vascular model consisting, at a minimum, of a guide wire, guiding catheter and a vessel model where the stent can be deployed. Withdrawal force is measured by fixing the proximal hub to a load cell and retracting the system automatically at a given speed. Maximum withdrawal forces are typically measured when the balloon enters into the guiding catheter. The peak force is considered a measure of *retractability*. If the stent could not be deployed during a procedure, the balloon must be withdrawn with the loaded stent. The retractability can also be assessed based on measurements of deformations of the stents' outer contours. Low profile, smooth transitions between stent and balloon, as well as a firm fixation, are required to prevent stent loss. Section 8.6.1.3 of Ref. 10 (profile effect/flaring) addresses this issue with regard to stent outer contour after simulated use, that is, track, cross and push tests. The test is designed to measure the difference between the outer contour of the mounted stent and that of the folded balloon while bending the system for a defined radius. The measurements of deformations can be performed using calibrated microscope stages.

The *firmness of the crimping* represents an important criterion for safe intracoronary stenting. To prevent stent loss caused by sticking at sharp edges of a lesion, or at the tip of the guiding catheter, the withdrawal forces must be low. High crimp provides a safety buffer allowing the interventionalist to safely withdraw a system if the stent deployment strategy has to be changed. The measurement of stent dislodgment force requires a proper fixation of the stent to the clamp of a tensile test machine, without affecting the contact between stent and balloon. A number of different techniques are known, such as simulation of sharp edged narrowing or fixation by thin wires, to simulate a difficult withdrawal. In our experience, fixing the stent by adhesive tape to the grip and pulling the catheter to the distal or proximal direction provided reproducible and reliable results. The recorded force–distance curves allow measurement of the maximum force that can be applied before the stent will leave its original crimped position (stent dislodgement force), and the force required to pull the stent entirely from the balloon (maximum pull force). Both values are useful to assess the safety of stent systems during delivery or retraction in Ref. 10, Section 8.5.2.9 (dislodgement force). A comparison of dislodgement forces measured for stent systems without and after simulated use has been published previously.[14]

Another important component of safety and facility of stenting represents the *deflation time* of the stent expanding balloon, mostly determined by the cross-sectional area of the tube connecting the balloon hub to the balloon at the distal end of the catheter. Due to the recent trends toward low profile systems with outer profiles $<<1$ mm, the issue of safe deflation has regained importance. The measurement of deflation (and inflation) time must be conducted in an environment of 37°C water using typical clinical equipment (inflation devices). It is required by the standard to use a mixture of saline and radiopaque contrast medium as is used in the catheterization laboratories. The selection of contrast agent is critical because its viscosity is much higher than that of water or physiological saline solution, thus determining the time required to fill or empty the dilatation balloon. Typically, the inflation time is shorter than deflation

time. This can be explained by the high pressure gradient that is applied during inflation. The inflation time depends on the rate of increase of the pressure rise produced by the hand pump, reaching up to 30 bar in high pressure systems. During deflation, such a high pressure gradient exists only at the very beginning of deflation and reaches a theoretical minimum pressure of about −1 bar, compared to the atmospheric pressure corresponding to an absolute vacuum. A minimum amount of volume evacuated from the balloon will decrease balloon pressure to around zero or below, resulting in a low negative pressure difference driving the emptying of the balloon.

Characteristically, the main mechanical function of deployed stents is to prevent vessel wall recoil or collapse following dilatation, termed *support*. Based on the FDA recommendations,[13] radial stiffness and radial strength were defined as the change in stent diameter as a function of uniformly applied external radial pressure and the pressure at which the stent experiences irrecoverable deformation, respectively. In self-expanding stents, radial outward force, that is, force exerted against the vessel wall after deployment, should also be measured. However, little is known about the actual radial compressive forces acting on a stent following dilatation of stenoses. Considering arterial walls of healthy subjects, a compliance of 5–7% /100 mmHg appears a reasonable assumption based on earlier measurements.[17,18] These data help to estimate the loading of overdilated stents; the lower the vessel compliance, the higher the load at a given percentage of overexpansion. Taking a compliance of 5%/100 mmHg and an overexpansion of 10% related to the native vessel diameter, a pressure load of 200 mmHg (approximately 0.27 bar) shall be supported by the stent. Yet, atherosclerotic, frequently calcified, coronary artery walls may exhibit substantially larger radial forces to oppose stretching, compared to healthy vasculature. Radial overstretching of the coronary artery may also lead to a destruction of the wall architecture with consecutive partial or complete loss of radial compression forces leading to a collapse of the lumen. Thus, it is assumed that disrupted plaques shall likely exert only a low radial load on the stent comparable to or even lower than normal healthy vessel walls.

The measurement of the support function of stents can be performed using different methods, none of them as yet standardized. We have a long-year experience with radially applied loading of the stents. This method simulates a uniform and strictly radial load on the stents and is well suited for comparison of stent support function in many clinical cases. For this purpose, the stent is implanted in a thin tube (inner diameter $\approx$ outer stent diameter) and loaded by a stepwise increasing outer hydraulic pressure. The test tube is flexible enough not to shield the stent from the outer applied hydraulic pressure, but to separate the inner lumen of the stent from the surrounding water and thus enabling the loading. The diameter of the stent is measured at a predetermined section to evaluate stent deformation at increased loading. The pressure at which the stent can no longer withstand the outer pressure is called the collapse pressure and is the measure of radial strength. Collapse pressure values from 0.5 bar (at stent diameters of 3.0 mm) up to more than 2.0 bar have been measured in commercially available and clinically well established stents in the past. However, it has not yet been determined whether greater radial force of a stent, that is, higher collapse resistive pressure provides better clinical results, and acute and late patency rates.

Other methods are recommended to obtain data on the support function in case of nonuniform loading. Thus, the stent can be loaded between parallel plates of decreasing distance and parallel measurement of force–distance curves in a universal test machine. The load force at 10, 20 and 50% of stent deformation will provide the required measures of support function. For comparison of stents of different length, normalization with respect to stent length is useful to provide the force in units of N/mm of stent length. This method can be modified by using smaller plates or other shapes to simulate focal lesion interaction. Unfortunately, focal loading has not yet been fully standardized.

Besides support *scaffolding*, prevention of protrusions and dislodgments of the fractured, fissured or dissected structures following dilatation is critical for safe and successful stenting. This critical stent function may be assessed under different conditions. Thus, a uniform distribution of stent struts is needed to provide a homogenous support to the entire stented vessel segment, preventing protrusions of lesion flaps between the stent struts. In DES, a homogenous distribution of the eluting drug following stent expansion is also critical.

The maximum achievable vessel wall or surface coverage depends on the ratio between the crimped and expanded stent diameter. Assuming no strut overlap and no gaps between the stent struts in the crimped state, the vessel wall coverage (metal-to-artery ratio) is

$$m = \frac{d_{\text{crimped}}}{d_{\text{expanded}}} \cdot 100\%$$

where d_{crimped} and d_{expanded} correspond to the diameters in the crimped and expanded state. Thus, expanding a stent from 0.9 to 3.0 mm outer diameter a maximum metal-to-artery ratio of 30% is possible. In practice, the ratio depends on the specific stent design. Typical values of 3.0 mm stents are about 12–15%. This ratio does not consider the uniformity of strut distribution. This could be obtained by using the theoretical construction data of stent design typically available only to the manufacturers or analysis based on imaging of expanded stents. An applicable indirect method requires knowledge of stent material density and measurement of the stent total mass and strut thickness.

Nonuniform strut distribution may be advantageous in a number of specific implantation settings, such as bifurcations, branching, ostial location, and so forth. The appropriateness of specific stent designs dedicated to special procedures requires testing in anatomical vessel models under simulated conditions. However, standardization has yet to be established.

The knowledge of stent shortening during deployment is important for exact sizing. The degree of shortening is a function of stent design as well as the interaction of the stent with the expanding balloon. In the latter case, it has to be considered that most balloons are compliant to some degree and increase, not only in diameter, but also in length during inflation, forcing the stent to overstretch and to get longer. These changes in strut geometry and stent length may become clinically important if a precise stent placement and optimum coverage of the entire target lesion are critical. Endothelial cell proliferation or imprecise positioning may require deployments of additional stents, associated with higher restenosis rates while increasing procedural risk and cost.

Finally, long-term mechanical stability and resistance to fracture appear critical for stent longevity and patient safety. Currently, long-term evaluation is performed using pulsatile fatigue/durability testing simulating at least 10 years of *in vivo* service. This is equivalent to 380–400 million load cycles and requires accelerated testing at frequencies of 60 Hz and higher. Two different approaches are established. One, ASTM F 2477-07,[19] is intended to expose the stent to physiologically relevant vessel diameter changes (about 5% of vessel diameter) while the stent is mounted within a vessel-mimicking test tube and loaded by simulating the mean and pulsatile blood pressure within the tube. In response to this varying inner pressure, the tube expands and shrinks and thus exposes the stent to a cyclic load. The functionality of the test depends on the stent remaining in close contact to the inner wall of the test tube. This requirement, among others, limits the use of high test frequencies. A modification of this approach uses stiffer tubing than natural vessels, in combination with higher pulse pressure amplitudes, to obtain comparable diameter changes.

The second test method[20] uses thin and flexible polymer tubes. The stent is implanted into such a tube, achieving an initial static pressure load from the overstretched vessel/tube wall. In contrast to the previous method, the hydraulic pressure is applied from outside the tubing to the stent. The loading on the stent consists of an additional static component and a dynamic component to reproduce a worst-case physiological pressure difference of about ± 40 mmHg. Due to the outer pressure loading, permanent contact between the stent and tubing is achieved. It was shown that coronary stents could be tested with adequate diameter changes at loading frequencies of up to 100 Hz.[21]

Fatigue testing has always to be supported by finite element calculations to estimate worst-case conditions of the stent and to forecast challenging structures with critical stress. Similar to other performance characteristics, virtually no data on long-term mechanical integrity testing of coronary stents is available in the literature. Clinical observation is not adequate to evaluate the long-term mechanical integrity. First, because there is limited imaging capability to resolve details of the individual strut structures of coronary stents. Second, mechanical loading is assumed to be much less challenging in coronary vessels than in specific peripheral vasculature such as renal, superficial femoral artery, or infrapopliteal regions.

Stent and balloon dimensions are displayed on the label of the stent system. This includes stent length (expanded), stent nominal diameter at NP, shaft working length and profile of overall tubing. The stent diameter is defined as the inner diameter of the stent.[12] The international standard lacks such a definition but refers to the established ASTM standard.[10] However, in practice the inner diameter of a stent is more difficult to measure with the same accuracy that has been customary in the measurements of the outer diameter. To circumvent this inconvenience, in practice, the outer diameter is usually measured and the twofold strut thickness is subtracted. Consequently, the stent diameters at given balloon pressures, as indicated in the compliance diagrams, should reflect the inner diameter of the stent at any given pressure. Considering the fact that all balloon expandable stents display some degree of elastic recoil—ranging between 2 and 6% of nominal stent diameter, depending on stent design and material—the final stent diameters are definitely smaller than the values typically indicated. The diameter underestimates may be as large as 0.1–0.2 mm. This approximation does not take into account any further stent compression due to the loading of the surrounding vessel. Measurements of the outer stent diameters of different stent designs showed deviations ranging from -0.097 to $+0.294$ mm, which corresponds to more than 0.3 mm, or approximately 10% of the nominal stent diameter (Table I).[22] These measurements suggest that the methods used to generate the data provided by the manufacturers may not be always accurate. In addition to the customary labeling numbers, indicating an accepted tolerance, standardized methods of measurements should be indicated to avoid errors.

Behavior of stents: computational analysis

In addition to the properties related to stent delivery, the concepts of firmness of crimping, support, scaffolding, and shortening, discussed above, are related to the deployment or postdeployment behavior of the stents. Because stent geometries are complex, finite element models have been used to calculate stresses in the stent struts, to predict their deployment and postdeployment behavior, and to analyze stent design. Finite element models are generally used to predict the permanent deformation and elastic recoil associated with deployment, as well as stresses experienced as the stent functions *in vivo*. In finite element models, it is possible, in principle, to model the stent geometries, the balloon geometries, the interaction between the balloons and stents, the deployment of the stent, and the interaction between the stent and the lesion. By doing so, researchers are able to predict the stent's behavior.

In his comprehensive review of stent properties, Lewis[4] indicates that there are relatively few studies, experimental, analytical, or numerical, of stent behavior. His suggested focus for future research is on deployment or postdeployment characteristics of stents. Deployment of intracoronary stents requires permanent (plastic) deformation of the stent, usually through application of forces from inflation of the balloon. Finite element analyses of the stents have included modeling: the expansion and plastic deformation

during deployment,[23] optimization of the stent design,[24–27] expansion of a stent in a curved vessel,[28] nonuniform stent expansion,[29] stent geometry after deployment, such as "dogboning,"[30,31] the stresses induced by systolic/diastolic pressures,[32] drug elution,[27,33] arterial injury,[34,35] hemodynamics,[36] fatigue life,[37] and self-expanding stents.[38]

There are some, although few, reports that examine behavior using both numerical and experimental methods, and compare the results.[35–37] These studies are critical to validate the finite element method's predictions, and to understand the effect of the assumptions made in the modeling. We are not aware of any numerical modeling studies of stent behaviors as they are delivered to the lesion site or of any studies with complementary numerical and experimental measurements of stent behavior during delivery.

This list is not intended to be exhaustive nor necessarily comprehensive; a critical review of the numerical studies is beyond the scope of this article. The successful modeling of different stent behaviors using computational methods, such as finite element analysis, provides a more complete understanding of the mechanical behavior of stents by allowing the many parameters associated with stent function to be explicitly addressed. Further investigations will undoubtedly continue to provide valuable information for improving stent performance. Often, these analyses represent idealized conditions, which may or may not be realized, or realizable, by the clinician. We believe that with the availability of current computational technology and power, numerical modeling shall aid stent selection and implantation strategies used by the clinicians. Improved matching between the biomechanical behavior of stents and vessel wall properties is likely to reduce both local traumata such as edge dissections and plaque shifts and the incidence of distal embolizations responsible for microvascular injuries.

Biomechanical properties of coronary artery lesions

The typical dimensions of normal coronary arteries include wall thickness, ranging between 0.55 and 1.0mm,[39] luminal diameter, ranging between 1 and 5 mm[40] and length, ranging between 1 and 25mm (left main), 10 and 13 cm (left anterior descending), 6 and 8 cm (left circumflex), and 12 and 14 cm (right coronary artery).[41] In coronary artery disease, more than a fourfold increase in wall-thickness with atherosclerosis has been reported.[39]

Several mathematical models have been proposed and studied to describe biomechanical behavior of arteries,[42–44] yet so far none has been universally accepted. Based on the nonlinear mechanical behavior of the coronary artery walls, these models assume that the walls are a hyperelastic solid. However, to date no existing model can universally predict the behavior of the coronary arteries under all loading conditions *in vivo*, nor does any model completely account for all loading components (e.g., residual stress).[45] In fact, the parameters used in the mathematical models may even not be related to observed phenomena, nor have readily interpreted physical meaning. Even though mathematical models are still under development, it has become clear that the microstructure of the coronary arterial wall plays a pivotal role in their biomechanical behavior. The biomechanical behaviors of the coronary artery intima, media and adventitia have been studied *ex vivo*[46]; however, the clinical importance of these observations in coronary interventions has yet to be established. Thus, although various descriptions of the behaviors of normal arteries have been proposed, none capture the relationship between structure and function accurately.

Alternatively, the behavior of both arteries and lesions can be described with equations that are descriptive of experimental results (i.e., stress vs. stretch or strain measurements). Such mathematical descriptions may reproduce the experimental data,[47] but may not represent material properties; the experimental data are necessarily dependent on the experimental parameters (e.g., specimen size, thickness, etc.). Therefore, such descriptions are useful to compare behaviors of lesions, but only when the experimental parameters are consistent.

In general, the mechanical response of the coronary arterial lesions (CAL) to mechanical loads may be divided into two broad categories: permanent (inelastic or plastic) deformations and nonpermanent or recoverable (elastic) deformations. Whether or not the lesions deform permanently depends on both the stresses applied by the balloons and the stents, and the material mechanisms available. The mechanisms of both elastic and plastic deformations depend on the materials that constitute the lesions, that is, the type of lesion. In general, lesions exhibit nonlinear behavior. Calcified, fibrotic, soft, and mixed CAL can be roughly distinguished.[48] The extremely rigid, hard, and highly calcified plaques appear to be particularly prone to fracturing, fissuring, long longitudinal dissections, and plaque shifts. Following high pressure inflations, the disruptions of these brittle plaques may interfere with the subsequent stent placements and strut appositions. Stiff fibrotic plaques may prevent a full stent expansion enforcing recoils. Soft, pliable plaques, particularly if associated with large necrotic cores, may encourage formation of tissue flaps, protrusions of debris and distal embolizations when stented. Yet, due to their complexity, the mechanical behavior of CAL remains poorly defined *in vivo*, without or with stenting.

Besides acute responses to mechanical deformations, time responses of composite CAL are critical for the outcome of interventions such as plain balloon dilatations or stenting with bioabsorbable materials. For engineering materials, the "creep" or "stress relaxation" behaviors due to viscoelastic properties can be easily determined. The viscoelastic material may initially exhibit an elastic deformation when loaded, but over time, that deformation may become permanent or plastic. This observation has been exploited in the design of BAS, where over time, the coronary artery will either remodel and recoil or its tendency to recoil will vanish, making the stent in the later course following implantation unnecessary. Some CAL may not mechanically stabilize over time following initial plastic deformation. In fact, little is known about the long-term viscoelastic responses of diseased tissue.

The stiffness of a lesion may be broadly defined as the resistance to deformation under an applied load. Since vascular

tissue, including lesions, show nonlinear behavior, there is no single parameter to describe the stiffness. In fact, the nonlinear behavior shows that the stiffness increases as the loading, and hence deformation, increases. Calcified lesions appear to be the stiffest, with the stiffness likely dependent on the extent of calcification. The calcified lesions also recover to their original state after loading is removed. The viscoelastic behavior of calcified lesions will, however, depend not only on the relative amount of calcified and noncalcified (e.g., collagen) components, but also on the biomechanical properties of the embedding coronary artery walls.

To complicate the matter further, it must be acknowledged that little is known about the long term response of calcified lesions under prolonged load (e.g., from a stent). Previous results[49] may indicate that, under loads that produce different viscoelastic responses in fibrous or atheromatous lesions, calcified lesions may be subject to permanent deformation. However, calcified lesions must likely be fractured before they exhibit significant permanent deformations. If calcified lesions are not sufficiently deformed, then opening of the lumen probably occurs through mechanisms other than lesion remodeling, that is, overstretching of the lesion-free arterial wall.

At the other extreme of mechanical behavior, atheromatous lesions, with necrotic cores, are likely the most easily deformed. Under the same loading conditions as for calcified lesions, atheromatous plaques stretch more than the calcified plaques by a factor of more than 20.[49] Experimental data show also that the deformations are inelastic, and the original state of the lesion is not recovered after loads are removed. In addition, the atheromatous lesions can be further deformed by renewed application of forces.

Fibrous lesions show an intermediate stiffness between the calcified and atheromatous. Given our informal definition of stiffness, they are approximately 10 times less stiff than calcified plaques, but approximately twice as stiff as atheromatous plaques.[49] They exhibit inelastic behavior, but in contrast to the atheromatous lesions, reach their deformation limit sooner, since they have no necrotic material to redistribute.

For each type of lesion, we must also consider the forces that the lesions apply back on the stent, which are expressed by the lesion's tendency to recoil. The tendency to recoil, in turn depends on both the lesion's stiffness and the mechanisms of permanent deformation. It is likely that all lesions exhibit some combination of elastic (recoverable) and inelastic (permanent) deformation when subject to mechanical interventions. In another of the few studies of the inelastic behavior of plaques, the measured permanent deformation, upon unloading, had no correlation with the clinical classification of the lesion.[50] Regardless of the composition, the greater the permanent deformation, the less force the lesion will likely apply back on the stent.

FUTURE PERSPECTIVES

Complications of stenting are relatively rare, yet given the large number of stenting procedures performed, their overall incidence cannot be neglected.[51] Besides restenosis, thrombosis, strut malapposition and incomplete strut endothelialization, several clinical problems are important:

- *failed stenting* denoting the inability to deliver the stent to the target site or to deploy the stent fully,
- *difficult stenting* referring to the necessity of using accessory techniques such as multiple predilatations of nontarget sites, use of additional guide-wires and/or use of use of undue forces to place the stent,
- *extended stenting* referring to the unintended deployment of multiple stents in a target lesion or adjacent secondary targets, frequently associated with strut damage and deformation of stent geometry,
- *complicated stenting* referring to suboptimal results due to undersizing, stent malpositioning and side branch (>2 mm diameter) closure,
- *injurious stenting* referring to stenting associated with immediate or delayed complications such as mechanical vessel obstruction or closure, no-reflow following stent deployment in a previously opened vessel, edge dissections, longitudinal dissections, perforations, aneurysm formation, and stent loss.

In the future, further improvement of the clinical outcome of intracoronary stenting, through stent selection based on knowledge of stents' biomechanical properties, and even individual stent–lesion matching, appears not to be a vain hope but a necessity to further improve clinical outcomes. To achieve these aims, four major steps need to be accomplished. First, standard methodologies for measuring the biomechanical properties of stents and SDS must be developed; examples and some proposed methods have been provided in this article. Second, industry needs to adopt these methods and market their stent products along with the disclosure of the relevant nonproprietary biomechanical data. Third, biomechanical interactions between stents and lesions need to be better studied and understood. Fourth, the results of steps 1–3 need to be clinically applied. Further advancements of the state of the practice and art of intracoronary stenting are an important future goal of the interventional community.

CONCLUSIONS

Introduction of intracoronary stents has markedly improved the safety and the outcome of coronary interventions. However, with the broad use of stents, even the rare adverse effects have become clinically and economically relevant. Optimal selection of stents based on standardized and objective criteria will further improve the outcome of intracoronary stenting in the future. Critical steps to achieve this aim were briefly outlined.

REFERENCES

1. Wessely R. New drug-eluting stent concepts. Nature Rev Cardiol 2010;7:194–203.
2. Stone GW, Leon MB, editors. Textbook of Coronary Stenting. New York: CRF Publications; 2004.

3. Lanzer P, Gijsen FJH, Topoleski LDT, Holzapfel GA. Call for standards in technical documentation of intracoronary stents. Herz 2010;35:27–33.
4. Lewis G. Review: Materials, fluid dynamics, and solid mechanics aspects of coronary artery stents: A state-of-the-art review. J Biomed Mater Res Part B: Appl Biomater 2008;86B:569–590.
5. Verheye S, Grube E, Ramcharitar S, Schofer JJ, Witzenbichler B, Kovac J, Hauptamm KE, Pierfrancesco A, Wiemer M, Lefevre T, Serruys PW, van Geuns RJ. First in man (FIM) study of the Stentys TM bifurcation stent-30 days results. EuroIntervention 2009;4:566–571.
6. Kastrati A, Mehilli J, Dirschinger J, Dotzer F, Schuhlen H, Neumann F-J, Fleckenstein M, Pfafferott C, Seyfarth M, Schomig A. Intracoronary stenting and angiographic results: strut thickness effect on restenosis outcome (ISARSTEREO) trial. Circulation 2001;103:2816–2821.
7. Simon C, Palmaz JC, Sprague EA. Endothelial cell migration onto metal stent surfaces under static and flow conditions. J Long Term Eff Med Implants 2000;10:143–151.
8. Briguori C, Nishida T, Anzuini A, di Mario C, Grube E, Colombo A. Emergency polytetrafluoroethylene-covered stent implantation to treat coronary ruptures. Circulation 2000;101B:3028–31.
9. Grube E, Buellesfeld L, Neumann F-J, Verheye S, Abizaid A, McClean D, Mueller R, Lansky A, Mehran R, Costa R, Gerckens U, Trauthen B, Fitzgerald PJ. Six-month clinical and angiographic results of a dedicated drug-eluting stent for the treatment of coronary bifurcation narrowings. Am J Cardiol 2007; 99:1691–1697.
10. ISO 25539-2: 2009-08, Cardiovascular implants—Endovascular devices—Part 2: Vascular stents; 2009. http://www.iso.org/iso/isoupdate_march09.pdf (accessed 05.30.2010).
11. EN 12006-3: 2009-08, Non-active surgical implants—Specific requirement for heart and vascular implants—Part 3: Endovascular implants; 2009. http://www.beuth.de/langanzeige/DIN+EN+12006-3/118460267.html (accessed 05.30.2010).
12. ASTM 2081-06: Standard guide for characterization and presentation of the dimensional attributes of vascular stents; 2006. http://www.astm.org/SNEWS/NOVEMBER_2006/actf_nov06.html (accessed 05.30.2010).
13. Guidance for industry and FDA staff non-clinical engineering tests and recommended labelling for intravascular stents and associated delivery systems. http://www.fda.gov/MedicalDevices/DeviceRegulationandGuidance/GuidanceDocuments/ucm071863.htm (accessed 05.30.2010).
14. Schmidt W, Schmitz, K-P. Devices. In: Lanzer P, editor. Mastering of Endovascular Techniques—A Guide to Excellence. Philadelphia: Lippincott William & Wilkins; 2006. pp 114–135.
15. Rieu R, Barragan P, Garitey V, Roquebert PO, Fuseri J, Commeau P, Sainsous J. Assessment of the trackability, flexibility, and conformability of coronary stents: a comparative analysis. Cathet Cardiovasc Interv 2003;59(4):496–503.
16. Schmidt W, Lanzer P, Behrens P, Topoleski LDT, Schmitz K-P. A comparison of the mechanical performance of seven drug-eluting stent systems. Cathet Cardiovasc Interv 2009;73:350–360.
17. Alfonso F, Macaya C, Goicolea J, Hernandez R, Segovia J, Zamorano J, Bañuelos C, Zarco P. Determinants of coronary compliance in patients with coronary artery disease: an intravascular ultrasound study. J Am Coll Cardiol 1994;4:879–884.
18. Nakatani S, Yamagishi M, Tamai J, Goto Y, Umeno T, Kawaguchi A, Yutani C, Miyatake K. Assessment of coronary artery distensibility by intravascular ultrasound. Circulation 1995;91:2904–2910.
19. ASTM F 2477-07: Standard test methods for in vitro pulsatile durability testing of vascular stents; 2007.
20. Schmitz K-P, Behrens P, Schmidt W, Behrend D, Kaminsky J, Lootz D, Enzenross P. Anordnung und Verfahren zur Prüfung von Gefäßimplantaten [Test set for blood vessel implants uses fluid filled cavity to apply dynamic test pressure for life test]. Patent DE 19903476.1; 1999.
21. Schmidt W, Kaminsky J, Behrens P, Schmitz K-P. Stentdeformation bei beschleunigter radialer Gefäßbelastung in Abhängigkeit von der Belastungsfrequenz. Biomedizinische Technik 2003 Erg S;48:68–69.
22. Schmidt W, Behrens P, Schmitz K-P. Biomechanical aspects of potential stent malapposition at coronary stent implantation. In: Dössel O, Schlegel WC, editors. WC2009, IFMBE proceedings 25/XI; 2009. pp 136–139.
23. Gervaso F, Capelli C, Petrini L, Lattanzio S, Di Virgilio L, Migliavacca F. On the effects of different strategies in modeling balloon-expandable stenting by means of finite element method. J Biomech 2008;41:1206–1212.
24. Timmins LH, Moreno MR, Meyer CA, Criscione JC, Rachev A, Moore JE Jr. Stented artery biomechanics and device design optimization. Med Biol Eng Comput 2007;45:505–513.
25. Kiousis DE, Gasser TC, Holzapfel GA. A numerical model to study the interaction of vascular stents with human atherosclerotic lesions. Ann Biomed Eng 2007;35(11):1857–1869.
26. De Beule M, Mortier P, Carlier SG, Verhegghe B, Van Impe R, Verdonck P. Realistic finite element-based stent design: The impact of balloon folding. J Biomech 2008;41:383–389.
27. Pant S, Bressloff NW, Limbert G. Geometry parameterization and multidisciplinary constrained optimization of coronary stents. Biomech Model Mechanobiol 2012;11:61–82.
28. Wu W, Wang, WQ Yang, DZ Qi, M. Stent expansion in curved vessel and their interactions: A finite element analysis. J Biomech 2007;40:2580–2585.
29. Yang J, Liang MB, Huang N, Liu YL. Studying the non-uniform expansion of a stent influenced by the balloon. J Med Eng Technol 2010;34(5–6):301–305.
30. De Beule M, Van Impe R, Verhegghe B, Segers P, Verdonck P. Finite element analysis and stent design: Reduction of dogboning. Technol Health Care 2006;14:233–241, 233.
31. Wang WQ, Liang DK, Yang DZ, Qi M. Analysis of the transient expansion behavior and design optimization of coronary stents by finite element method. J Biomech 2006;39:21–32.
32. Donnelly EW, Bruzzi MS, Connolley T, Mchugh PE. Finite element comparison of performance related characteristics of balloon expandable stents. Comput Methods Biomech Biomed Eng 2007;10(2):103–110.
33. Migliavacca F, Gervaso F, Prosi M, Zunino P, Minisini S, Formaggia L, Dubini G. Expansion and drug elution model of a coronary stent. Comput Methods Biomech Biomed Eng 2007;10(1):63–73.
34. Zahedmanesh H, Lally C. Determination of the influence of stent strut thickness using the finite element method: implications for vascular injury and in-stent restenosis. Med Biol Eng Comput 2009;47:385–393.
35. Kiousis DE, Wulff AR, Holzapfel GA. Experimental studies and numerical analysis of the inflation and interaction of vascular balloon Catheter-stent systems. Ann Biomed Eng 2009;37(2):315–330.
36. Balossino R, Gervaso F, Migliavacca F, Dubini G. Effects of different stent designs on local hemodynamics in stented arteries. J Biomech 2008;41:1053–1061.
37. Li J, Luo, Q Xie, Z, Li Y, Zeng Y. Fatigue life analysis and experimental verification of coronary stent. Heart Vessels 2010;25:333–337.
38. Kim JH, Kang TJ, Yu WR. Mechanical modeling of self-expandable stent fabricated using braiding technology. J Biomech 2008;41:3202–3212.
39. Fayad ZA, Fuster V, Fallon JT, Jayasundera T, Worthley SG, Helft G, Aguinaldo G, Badimon JJ, Sharma SK. Noninvasive in vivo human coronary artery lumen and wall imaging using black-blood magnetic resonance imaging. Circulation 2000;102:506–510.
40. Dodge JT Jr., Brown G, Bolson EL, Dodge HT. Lumen diameter of normal human coronary arteries; influence of age, sex, anatomic variation, and left ventricular hypertrophy or dilation. Circulation 1992;86:232–246.
41. Waller BF, Schlant RC. Anatomy of the heart. In Schlant RC, Alexander RW, editors. The Heart, 8th ed. New York: McGraw-Hill; 1995. pp 84–86.
42. Chuong C, Fung Y. Three-dimensional stress distribution in arteries. J Biomech Eng 1983;105:268–274.
43. Gleason RL, Hu JJ, Humphrey JD. Building a functional artery: Issues from the perspective of mechanics. Front Biosci 2004;9:2045–2055.
44. Haslach H. Nonlinear viscoelastic, thermodynamically consistent, models for biological soft tissue. Biomech Model Mechanobiol 2005;3(3):172–189.
45. Humphrey J. Mechanics of arterial walls: Review and directions. Crit Rev Biomed Eng 1995;23:1–162.

46. Holzapfel GA, Sommer G, Gasser CT, Regitnig P. Determination of layer-specific mechanical properties of human coronary arteries with non-atherosclerotic intimal thickening, and related constitutive modeling. Am J Physiol Heart Circ Physiol 2005;289:H2048–H2058.
47. Wagner DR, Reiser KM, Lotz JC. Glycation increases human annulus fibrosis stiffness in both experimental measures and theoretical predictions. J Biomech 2006;39:1021–1029.
48. Topoleski LDT. Atherosclerotic lesions: mechanical properties. In: Lanzer P, Topol EJ, editors. PanVascular Medicine; Integrated clinical management. New York: Springer Verlag; 2002. pp 340–352.
49. Topoleski LDT, Salunke NV. Mechanical behavior of calcified plaques: a summary of compression and stress-relaxation experiments. Z Kardiol 2000;89(suppl 2):II/85–II/91.
50. Maher E, Creane A, Sultan S, Hynes N, Lally C, Kelly DJ. Inelasticity of human carotid atherosclerotic plaque. Ann Biomed Eng 2011;39(9):2445–2455.
51. Lanzer P, Prechelt L. Spelling out risk reduction strategies for intracoronary stenting. EuroIntervention 2008;3:622–626.